 

# Application of $^{57}$Fe Mössbauer Spectroscopy to a Study of the Difference in Interactions between Guest and Host Molecules among (*R*), (*S*) and Racemic Isomers for (2-Methylbutyl)-, (2-Phenylpropyl)- and (2-Phenylbutyl)ferrocenes Enclathrated in Deoxycholic Acid

**Satoru Nakashima,* Naoki Ichikawa†, and Tsutomu Okuda*,†**

Radioisotope Center and Department of Mathematical and Life Sciences, Graduate School of Science, Hiroshima University, Higashi-Hiroshima 739-8526

†Department of Chemistry, Graduate School of Science, Hiroshima University, Higashi-Hiroshima 739-8526

(Received January 9, 2002)

$^{57}$Fe Mössbauer spectroscopy was applied to determine the difference, if any, in the interactions between host and guest molecules among the (*R*)-, (*S*)- and racemic isomers for (2-methylbutyl)-, (2-phenylpropyl)- and (2-phenylbutyl)ferrocene-deoxycholic acid (DCA) clathrates. The (*S*) isomer is included into DCA, while the (*R*) isomer is not in the case of (2-phenylpropyl)ferrocene. There is no significant difference in the temperature dependences of the $^{57}$Fe Mössbauer spectra between the (*S*) and racemic isomers-DCA for (2-phenylpropyl)ferrocene. For 2-methylbutyl and 2-phenylbutyl derivatives, all isomers form DCA clathrates. $^{57}$Fe Mössbauer spectroscopy revealed a difference in the molecular motion of guest molecules in the DCA lattice among them. For the 2-phenylbutyl derivative, the (*S*) isomer-DCA clathrate has one solvated molecule per guest molecule, a racemic isomer-DCA 0.7 solvated molecule, while the (*R*) isomer includes no solvated molecule. There was a difference in the powder X-ray diffraction patterns among them. An interesting phase transition was observed in (*S*)- and racemic (2-phenylbutyl)ferrocenes-DCA, which was accompanied by a desolvation, and then a change of crystal structure to that of (*R*) isomer-DCA heated up to the same temperature. Such a phase transition was not observed in (*R*) isomer-DCA. $^{57}$Fe Mössbauer spectroscopy revealed that (*R*) isomer-DCA changes in lattice vibration around 160 K, while (*S*) isomer-DCA does not.

The chemistry of a chiral compound has been a main problem in chemistry for a long time. Optical resolution can be accomplished by using host-guest phenomena. In this case, the interaction between the host and guest molecules is an important problem.[1] Cholic acid (CA) and deoxycholic acid (DCA, which is shown in Scheme 1) have asymmetric carbons and form a variety of inclusion compounds with organic molecules.[2] CA and DCA have a possibility to achieve the optical resolution of a guest molecule. Although the optical resolution of lactones by an inclusion method using cholic acid as a host[3] and the chiral discrimination of 1-phenylethylamine by diastereomeric salt formation with cholic acid[4] are reported, there has been no report about the optical resolution using deoxycholic acid as a host.

$^{57}$Fe Mössbauer spectroscopy is a useful technique to know the molecular motion in inclusion compounds.[5] Recently, the present author et al. applied $^{57}$Fe Mössbauer spectroscopy to the molecular motion of ferrocene (FcH) in the DCA channel.[6] The existence of precession was confirmed, and it was newly suggested by using $^{57}$Fe Mössbauer spectroscopy that an anisotropic vibration of the FcH molecule is coupled with the precession. These findings do not contradict the results of NMR.[7] The present authors also reported that the motions in the DCA lattice are restricted by introducing a halogen atom to the ferrocene molecule.[8] The important thing is that the interaction between the host and guest molecules has a connection with

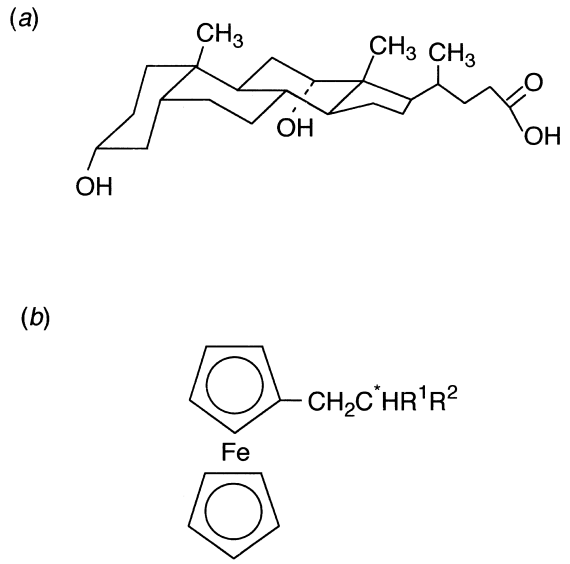


Scheme 1. (a) Deoxycholic acid (DCA). (b) (2-Methylbutyl)ferrocene (**1**) ($R^1$ = Me, $R^2$ = Et), (2-phenylpropyl)ferrocene (**2**) ($R^1$ = Ph, $R^2$ = Me), (2-phenylbutyl)ferrocene (**3**) ($R^1$ = Ph, $R^2$ = Et).

the molecular motions of the guest, which can be detected by using $^{57}$Fe Mössbauer spectroscopy.

The DCA may interact with a guest molecule of ferrocene derivatives having an asymmetric carbon in the substituent. The interaction is expected to be different between (*R*) and (*S*) isomers, since DCA has asymmetric carbons, even though both isomers can be included in the DCA lattice. Such a difference can be detected as a difference in the motion of guest molecules by using $^{57}$Fe Mössbauer spectroscopy. In the present study, $^{57}$Fe Mössbauer spectroscopy was applied to determine the difference in the interaction between guest and host molecules among the (*R*)-, (*S*)- and racemic isomers for (2-methylbutyl)-(**1**), (2-phenylpropyl)-(**2**) and (2-phenylbutyl)ferrocene (**3**) (Scheme 1) enclathrated in DCA.

## Experimental

**Syntheses.** All ferrocene derivatives in the present study were synthesized from ferrocene by acylation and its reduction. The acid chlorides for the acylation were synthesized by using thionyl chloride in DMF from the corresponding acid. We refer to the ferrocene derivatives synthesized from DL-, (*S*)- and (*R*)-2-phenylpropionyl chloride and phenylbutyryl chloride for the acylation as racemic, ((*R*)- and (*S*)-2-phenylpropyl)ferrocene and racemic, ((*R*)- and (*S*)-2-phenylbutyl)ferrocene, respectively, while from DL- and (*S*)-2-methylbutyryl chloride as racemic and ((*S*)-2-methylbutyl)ferrocene, respectively. The samples were separated by using alumina column chromatography. $^1$H NMR (500 MHz, $CDCl_3$) **1**, $\delta$ 4.11–4.23 (9H), 2.22–2.49 (2H), 1.38–1.46 (2H), 1.14–1.19 (1H), 0.88–1.02 (6H). **2**, $\delta$ 7.14–7.29 (5H), 3.87–4.16 (9H), 2.69–2.72 (2H), 2.54–2.55 (1H), 1.19–1.20 (3H). **3**, $\delta$ 7.07–7.27 (5H), 3.78–4.03 (9H), 2.59–2.68 (2H), 2.45–2.49 (1H), 1.49–1.73 (2H), 0.71–0.74 (3H). Powdered inclusion compounds were obtained from a methanol solution of 1:2 of the guest and host. The compounds were confirmed by powder X-ray diffraction patterns and elemental analyses. The powder X-ray diffraction patterns are not superpositions of patterns for the guest and host molecules. The powder patterns revealed that the crystal structures in **1**- and **2**-DCA clathrates are similar to each other, while the crystal structure of **3**-DCA clathrates shows a variety of types, depending on the isomer. The elemental analyses and thermal analyses for **3**-DCA suggest that (*S*) and racemic isomer-DCA include one molecule and 0.7 molecule of MeOH per guest molecule, respectively, although (*R*) isomer-DCA includes none of MeOH. Found for (*S*)-**1**-DCA: C, 72.32; H, 9.88%. Found for racemic **1**-DCA: C, 72.44; H, 9.74%. Calcd for $C_{24}H_{40}O_4 \cdot 1/2(C_{15}H_{20}Fe)$: C, 72.66; H, 9.70%. Found for (*S*)-**2**-DCA: C, 73.76; H, 9.15%. Found for racemic **2**-DCA: C, 73.98; H, 8.90%. Calcd for $C_{24}H_{40}O_4 \cdot 1/2(C_{19}H_{20}Fe)$: C, 73.86; H, 9.27%. Found for (*S*)-**3**-DCA-MeOH: C, 72.75; H, 9.67%. Calcd for $C_{24}H_{40}O_4 \cdot 1/2(C_{20}H_{22}Fe \cdot CH_4O)$: C, 72.98; H, 9.41%. Found for racemic **3**-DCA–0.7MeOH: C, 73.14; H, 9.46%. Calcd for $C_{24}H_{40}O_4 \cdot 1/2(C_{20}H_{22}Fe \cdot 0.7CH_4O)$: C, 73.29; H, 9.38%. Found for (*R*)-**3**-DCA: C, 73.76; H, 9.36%. Calcd for $C_{24}H_{40}O_4 \cdot 1/2(C_{20}H_{22}Fe)$: C, 74.01; H, 9.34%.

**Physical Measurements.** Powder X-ray diffraction patterns were observed by a Rigaku Rad-B system using Cu-$K\alpha$ radiation with a graphite monochrometer at room temperature.

A $^{57}$Co(Rh) source moving in a constant-acceleration mode was used for $^{57}$Fe Mössbauer spectroscopic measurements. Variable-temperature $^{57}$Fe Mössbauer spectra were obtained by using a Toyo Research spectrometer and a continuous-flow cryostat. The Mössbauer parameters were obtained by least-squares fitting to Lorentzian peaks. The isomer shift values are referred to metallic iron.

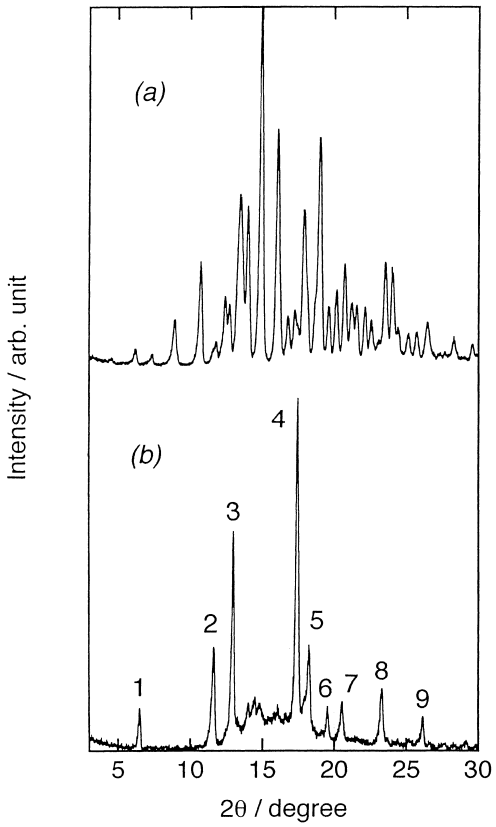


Fig. 1. Powder X-ray diffraction patterns for (a) DCA and (b) ((*S*)-2-methylbutyl)ferrocene-DCA clathrate. The indices obtained using the orthorhombic lattice constants of FcH-DCA are: 1(010), 2(310), 3(020), 4(510), 5(420), 6(130), 7(321), 8(430), 9(530).

A differential thermal analysis (DTA) was carried out using a home-built apparatus in the range of 100 to 400 K. The heating and cooling processes of the sample were repeated twice. The thermal weight loss was measured using a weighing bottle. After the bottle was heated up to a given temperature and cooled to room temperature in a desiccator, the weight was measured at room temperature.

## Results and Discussion

**(2-Methylbutyl)ferrocene-DCA and (2-Phenylpropyl)-ferrocene-DCA Clathrates.** Figure 1 shows the powder X-ray diffraction patterns for DCA and (*S*)-**1**-DCA clathrate. The (*S*)- and racemic **1** are oily substances. It can be easily seen that the pattern of the (*S*)-**1**-DCA is different from that of DCA. The pattern of (*S*)-**1**-DCA is identical to that of racemic **1**-DCA, and is similar to that of ferrocene(FcH)-DCA. It is known that the ferrocene molecule is fixed in the DCA channel in the ratio 1:2, as determined by a single-crystal X-ray diffraction study.[9] The packing view[10] is shown in Scheme 2. The similarity of the patterns suggests that (*S*)-**1** is also included into the DCA lattice in a similar manner, and that the ratio of **1** to DCA is 1:2. The elemental analysis also supports this ratio. Therefore, the crystal structures of (*S*)- and racemic **1**-DCA are similar to that of FcH-DCA. Thus, the reflections of

Table 1. Crystal Data of (2-Methylbutyl)- and (2-Phenylpropyl)ferrocene-DCA Inclusion Compound

| Guest | $a$/Å | $b$/Å | $c$/Å | $V$/Å$^3$ |
|---|---|---|---|---|
| ((*S*)-2-Methylbutyl)ferrocene | 27.24(3) | 13.85(4) | 6.98(6) | 2633(25) |
| Racemic (2-methylbutyl)ferrocene | 27.32(3) | 13.92(4) | 7.01(6) | 2666(25) |
| ((*S*)-2-Phenylpropyl)ferrocene | 27.05(3) | 13.88(4) | 6.85(6) | 2572(24) |
| Racemic (2-phenylpropyl)ferrocene | 27.01(3) | 13.91(4) | 6.84(6) | 2570(24) |

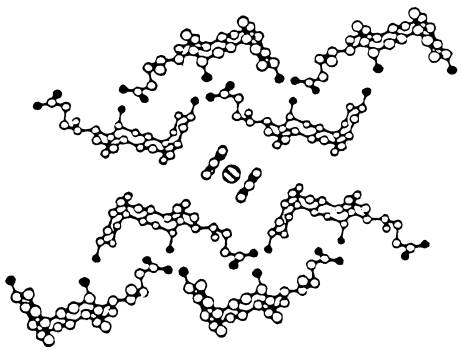

Scheme 2. Packing view of FcH-DCA taken from Ref. 10.

**1**-DCA can be indexed by using the orthorhombic lattice constant of FcH-DCA. The indices are also shown in Fig. 1. By using these indices we calculated the lattice constants of **1**-DCA; these are summarized in Table 1.

The (*S*)- and racemic **2** were included into DCA lattice in methanol solution, while the (*R*) isomer was not. The powder X-ray diffraction patterns of (*S*)- and racemic **2**-DCA clathrates are similar to each other, and are similar to those of **1**-DCA clathrates. The lattice constants are also summarized in Table 1. The fact that the racemic isomer is included into the DCA is very interesting, because the pure (*R*) isomer was not included into the DCA lattice. This phenomenon is explained by the assumption that the included (*S*) isomer slightly warps the lattice and, therefore, the (*R*) isomer can be included.

Figure 2 shows the typical variable-temperature $^{57}$Fe Mössbauer spectra of (*S*)-**1**-DCA clathrate. A ferrocene-like doublet is seen at all temperatures. Similar $^{57}$Fe Mössbauer spectra were observed in racemic **1**-DCA. The Mössbauer parameters for **1**- DCA, **2**- DCA, and **3**-DCA clathrates are summarized in Table 2. It can be easily seen from Fig. 2 that the symmetric doublets at low temperatures changed to the asymmetric ones at high temperatures. As can be seen in Table 2, the quadrupole splitting (QS) values at high temperatures are smaller than those at low temperatures. The S/N ratio becomes worse with increasing temperature. These trends were seen for the racemic isomer-DCA more significantly than that for the (*S*) isomer-DCA.

Measurements of the $^{57}$Fe Mössbauer spectra of **2**-DCA clathrates did not require a longer time compared with **1**-DCA clathrates. This finding is due to the difference in the recoil-free fraction. According to the Debye approximation at high temperatures, the logarithmic values of the recoil-free fraction and, therefore, of the total area intensity of the Mössbauer spectrum of their absorber, are expected to decrease linearly with increasing temperature. By comparing the temperature dependence of the logarithmic value of the area, the slopes of **2**-DCA clathrates are smaller than those of (*S*)- and racemic **1**-DCA clathrates. This shows that the Debye temperature is larger in **2**-DCA than in **1**-DCA. There was not a significant difference in the temperature dependence of the Mössbauer spectra between the (*S*) and racemic samples for **2**-DCA clathrates.

The temperature dependences of the area intensity ratio of the high-energy peak to the low-energy peak and of the QS value are shown in Figs. 3 and 4, respectively. For **1**-DCA clathrate, a symmetric doublet is observed in the range of 80 to ~240 K, while above ~240 K the doublet becomes asymmetric in the intensity. The asymmetry was increased with an increase in the temperature. For **2**-DCA clathrate, although a symmetric doublet was observed, a slight asymmetry began to be seen near room temperature. It is known that the asymmetry of the doublet is due to a preferred orientation and/or an anisotropy of lattice vibration (Gol′danskii-Karyagin effect).[11,12] The anisotropic recoil-free fraction is independent of the orientation of the sample. It is thought that the present asymmetry is due to the Gol′danskii-Karyagin effect, because the samples in the present study were powder and the asymmetry showed a temperature dependence. The effect of the preferred orientation does not change with a change of temperature. A similar temperature dependence was observed in ferrocene and its halogen-substituted derivatives enclathrated in DCA.[6,8] The electric-field gradient of ferrocene is reported to be positive.[13] It is also known that the introduction of substituents to FcH is less effective to the electric field gradient at the iron nucleus.[14] Therefore, the electric-field gradients in the present derivatives are safely assumed to be positive, as is the case of FcH. In this case ($V_{zz} > 0$), the increase in area ratio of the high-energy peak to the low-energy peak means that the vibration in a direction perpendicular to the molecular axis becomes more intense than that in a direction parallel to the axis at high temperatures ($<u_z^2> < <u_{x,y}^2>$) for an axially symmetric crystal, where $<u_z^2>$ and $<u_{x,y}^2>$ represent the mean-square amplitude parallel and perpendicular to the molecular axis, respectively.[15] We suppose here from the results of the powder X-ray diffraction patterns that the crystal structures are similar to that of FcH-DCA. In the FcH-DCA inclusion compound, DCA makes a channel in such a way that the molecular axis of ferrocene is perpendicular to the channel, as shown in Scheme 2.[9,10] In this case it can be supposed that the direction with a larger mean-square amplitude of vibration is the channel direction. It is thought that $<u_y^2>$ is the channel direction. Strictly speaking, axial symmetry does not hold in the present case, as is shown in Scheme 2. However, we can easily imagine the relations $<u_x^2> \approx <u_z^2>$ and $<u_y^2> >> <u_z^2>$ by considering the crystal structure. The temperature dependence of the asymmetry in the intensity in the present $^{57}$Fe Mössbau-

Table 2. Mössbauer Parameters

| *T*/K | IS[a)]/mm $s^{-1}$ | QS/mm $s^{-1}$ | Half width/mm $s^{-1}$ | Area ratio[b)] |
|---|---|---|---|---|
| ((*S*)-2-Methylbutyl)ferrocene-DCA | | | | |
| 298 | 0.443(27) | 2.293(28) | 0.36(5) | 1.43(17) |
| 270 | 0.447(14) | 2.332(15) | 0.31(3) | 1.27(9) |
| 240 | 0.489(1) | 2.374(1) | 0.293(1) | 1.007(4) |
| 200 | 0.477(14) | 2.357(3) | 0.36(3) | 1.04(7) |
| 160 | 0.499(5) | 2.384(4) | 0.26(1) | 1.06(4) |
| 80 | 0.522(3) | 2.401(4) | 0.255(6) | 1.04(2) |
| Racemic (2-methylbutyl)ferrocene-DCA | | | | |
| 298 | 0.466(33) | 2.131(34) | 0.31(6) | 1.62(25) |
| 270 | 0.467(31) | 2.285(34) | 0.40(7) | 1.21(15) |
| 240 | 0.491(18) | 2.381(21) | 0.30(4) | 1.06(11) |
| 200 | 0.503(11) | 2.370(13) | 0.35(3) | 1.07(6) |
| 160 | 0.495(14) | 2.402(16) | 0.39(3) | 1.12(7) |
| 80 | 0.517(5) | 2.405(5) | 0.312(9) | 1.01(3) |
| ((*S*)-2-Phenylpropyl)ferrocene-DCA | | | | |
| 298 | 0.441(1) | 2.400(1) | 0.229(1) | 1.08(1) |
| 270 | 0.455(8) | 2.407(9) | 0.33(2) | 1.14(5) |
| 240 | 0.469(5) | 2.418(5) | 0.306(9) | 1.02(3) |
| 200 | 0.487(1) | 2.430(1) | 0.286(1) | 1.06(1) |
| 160 | 0.501(3) | 2.436(4) | 0.367(6) | 1.03(2) |
| 120 | 0.513(2) | 2.438(2) | 0.290(3) | 1.04(1) |
| 80 | 0.521(2) | 2.431(2) | 0.258(2) | 1.04(2) |
| Racemic (2-phenylpropyl)ferrocene-DCA | | | | |
| 298 | 0.438(9) | 2.398(10) | 0.33(2) | 1.17(5) |
| 270 | 0.457(10) | 2.393(11) | 0.51(3) | 1.09(4) |
| 240 | 0.485(8) | 2.424(9) | 0.43(2) | 1.00(4) |
| 200 | 0.480(4) | 2.434(4) | 0.342(7) | 1.06(2) |
| 160 | 0.503(3) | 2.427(3) | 0.316(4) | 1.04(2) |
| 120 | 0.514(1) | 2.434(1) | 0.256(1) | 1.03(1) |
| 80 | 0.525(3) | 2.444(3) | 0.267(5) | 1.02(2) |
| ((*S*)-2-Phenylbutyl)ferrocene-DCA | | | | |
| 298 | 0.462(4) | 2.373(5) | 0.229(8) | 1.06(3) |
| 270 | 0.458(6) | 2.363(7) | 0.309(11) | 1.04(4) |
| 240 | 0.469(5) | 2.366(6) | 0.279(9) | 1.05(3) |
| 200 | 0.483(4) | 2.380(4) | 0.265(7) | 1.02(3) |
| 160 | 0.502(4) | 2.394(5) | 0.273(4) | 1.02(3) |
| 120 | 0.507(5) | 2.388(6) | 0.358(1) | 0.98(3) |
| 80 | 0.527(5) | 2.389(5) | 0.359(5) | 1.02(3) |
| ((*R*)-2-Phenylbutyl)ferrocene-DCA | | | | |
| 298 | 0.455(1) | 2.293(1) | 0.229(1) | 1.29(1) |
| 270 | 0.469(15) | 2.343(16) | 0.45(4) | 1.13(6) |
| 240 | 0.493(13) | 2.331(14) | 0.42(3) | 1.14(6) |
| 200 | 0.498(10) | 2.370(11) | 0.40(2) | 1.12(5) |
| 160 | 0.515(7) | 2.366(8) | 0.42(2) | 1.12(4) |
| 120 | 0.501(8) | 2.391(9) | 0.46(2) | 1.10(3) |
| 80 | 0.518(4) | 2.395(4) | 0.308(7) | 1.05(2) |
| Racemic (2-phenylbutyl)ferrocene-DCA | | | | |
| 298 | 0.437(63) | 2.350(68) | 0.48(7) | 1.28(28) |
| 270 | 0.485(25) | 2.348(28) | 0.33(5) | 1.10(14) |
| 240 | 0.467(12) | 2.321(13) | 0.27(3) | 1.09(8) |
| 200 | 0.482(8) | 2.366(8) | 0.26(2) | 1.14(5) |
| 160 | 0.517(9) | 2.365(10) | 0.34(2) | 1.09(5) |
| 120 | 0.508(5) | 2.384(5) | 0.233(8) | 1.11(4) |
| 80 | 0.515(6) | 2.384(6) | 0.322(11) | 1.03(3) |

a) Isomer shift data are reported with respect to iron foil.
b) Area intensity ratio of the high-energy peak to the low-energy peak in the doublet.

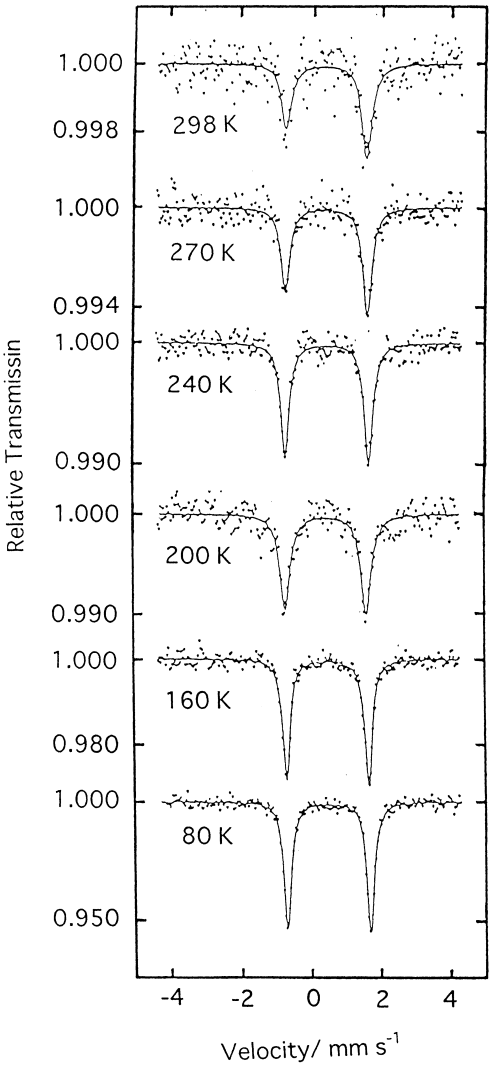


Fig. 2. Variable-temperature $^{57}$Fe Mössbauer spectra of ((*S*)-2-methylbutyl)ferrocene-DCA clathrate.

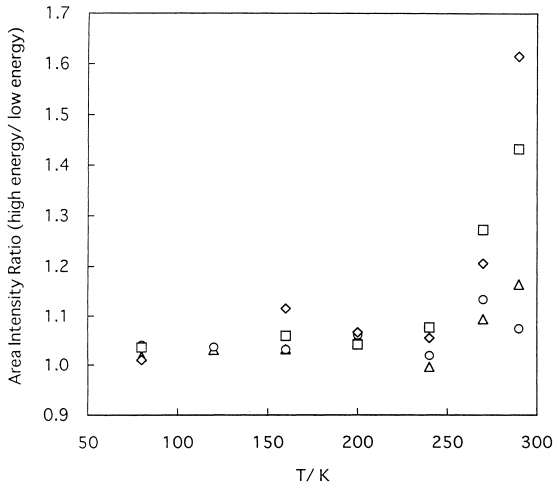


Fig. 3. Temperature dependence of area intensity ratio of the high-energy peak to the low-energy peak of (2-methylbutyl)ferrocene-DCA clathrate: □, (*S*) isomer-DCA; ◇, racemic isomer-DCA, and of (2-phenylpropyl)ferrocene-DCA clathrate: ○, (*S*) isomer-DCA; △, racemic isomer-DCA.

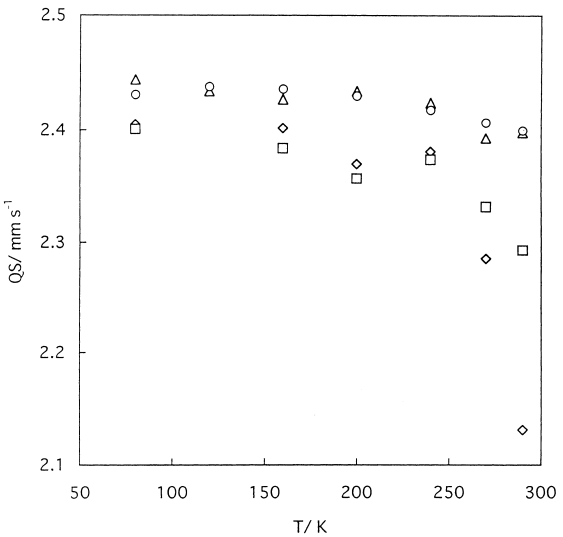


Fig. 4. Temperature dependence of the quadrupole splitting value of (2-methylbutyl)ferrocene-DCA: □, (*S*) isomer-DCA clathrate; ◇, racemic isomer-DCA, and of (2-phenylpropyl)ferrocene-DCA clathrate: ○, (*S*) isomer-DCA; △, racemic isomer-DCA.

er spectra is not inconsistent with the crystal structure.

It can be seen from Fig. 4 that the QS values are almost constant from 80 to ~240 K, and above ~240 K the value decreases abruptly for **1**-DCA clathrate. It is interesting that the onset temperature is almost equal to the temperature at which the asymmetry of the doublet began to be recognized. The decrease in the QS value can be explained by the precession of the guest molecules in the DCA channel in the same manner as the FcH molecule in the DCA lattice.[6] The electric-field gradient decreases in proportion to the cosine of the precession angle. It can be thought that the precession angle increases with increasing temperature. The QS value in the racemic isomer-DCA becomes smaller at room temperature than that in the (*S*) isomer-DCA for **1**-DCA clathrate, indicating that the precession angle of the former is larger than that of the latter. The QS value for **2**-DCA clathrates decreased more gradually with increasing temperature than that for **1**-DCA clathrates, as shown in Fig. 4. These findings suggest that the molecular motion of **2** in the DCA lattice is more restricted than that of **1** in the DCA lattice. This might reflect the interactions of the guest and host and/or guest and guest via a π–π interaction.

The relation between the molecular motion and the unit-cell volume has been reported in a series of halogen-substituted ferrocenes in DCA.[8] It is understandable that the molecular motion in DCA is more restricted in a smaller unit cell than in a larger one. From this point we checked the unit-cell volume of the present samples. Although the error is large, as can be seen from Table 1, the trend is that the unit cell volume of the (*S*) isomer is slightly smaller than that of racemic isomer for **1**-DCA clathrate. The volume of the (*S*) isomer is approximately equal to that of the racemic isomer for **2**-DCA. The similar volume suggests similar temperature-dependent $^{57}$Fe Mössbau-

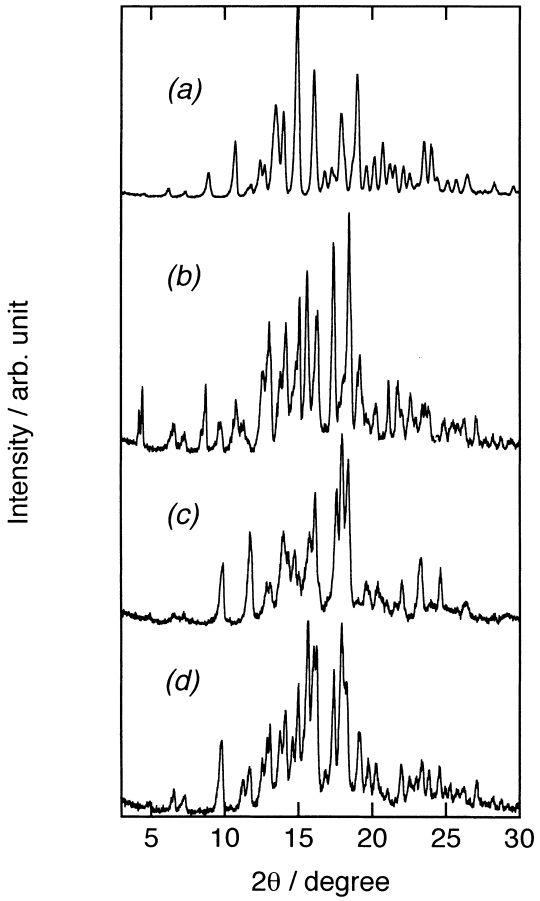


Fig. 5. Powder X-ray diffraction patterns for (a) DCA, (b) ((*S*)-2-phenylbutyl)ferrocene-DCA, (c) ((*R*)-2-phenylbutyl)ferrocene-DCA and (d) racemic (2-phenylbutyl)ferrocene-DCA clathrates.

er spectra. The unit-cell volumes of (*S*) and racemic **2**-DCA are smaller than those of (*S*) and racemic **1**-DCA, indicating that molecular motion is more difficult to occur for **2** than for **1** in DCA. Table 1 shows that the *a* and *c* axes for **2**-DCA clathrates are shorter than those for **1**-DCA clathrates. This finding suggests that the *a* and *c* axes are in an interaction direction.

**(2-Phenylbutyl)ferrocene-DCA Clathrate.** Figure 5 shows the powder X-ray diffraction patterns for DCA and (*R*)-, (*S*)- and racemic **3**-DCA clathrates. The patterns for **3**-DCA are different from that for DCA alone, indicating that inclusion phenomena occurred. However, there is a difference in the patterns among them. Also, they are different from those for **1**-DCA and **2**-DCA clathrates. An elemental analysis shows that the (*S*) isomer-DCA includes one molecule of MeOH per guest molecule, the racemic isomer-DCA includes 0.7 molecule of MeOH, while (*R*) isomer-DCA includes no MeOH molecule. The values of 1, 0.7 and 0 were determined by a thermal analysis, as shown in the next paragraph. It is interesting that the racemic isomer-DCA does not include 0.5 molecule of MeOH, but 0.7 molecule of MeOH. It can be thought that the included (*S*) isomer warps the host lattice, and therefore excess MeOH is included.

We measured DTA of these samples. The (*S*) isomer-DCA and racemic isomer-DCA showed a thermal anomaly, while

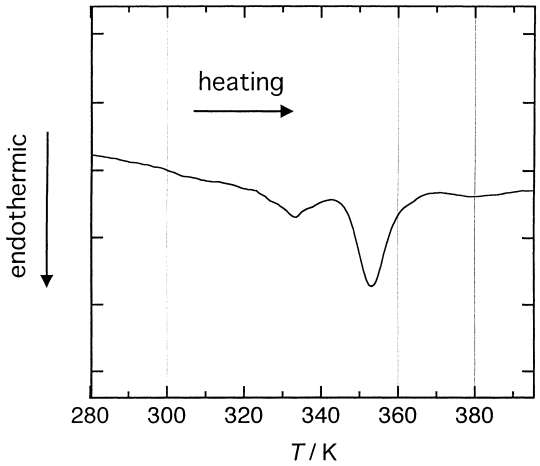


Fig. 6. DTA curve of ((*S*)-2-phenylbutyl)ferrocene-DCA clathrate.

the (*R*) isomer-DCA did not. Figure 6 shows the DTA curve of fresh (*S*) isomer-DCA. Two anomalies are seen around ~330 K and ~350 K. A fresh sample was heated first from room temperature up to 400 K, cooled down to 100 K, and then heated again up to 400 K. These processes were repeated. When the sample was cooled from 400 to 100 K, the corresponding exothermic peaks were not observed. In the second increasing process, the thermal anomaly was not observed. After heating a fresh sample at 343 and 400 K, we measured the powder X-ray diffraction patterns at room temperature, respectively. The results are shown in Fig. 7. The powder X-ray diffraction pattern of (*S*) isomer-DCA after heating at 343 K resembles that of the fresh one, although a slight change is detectable, perhaps because of a desolvation of the included MeOH molecule (see below). After heating at 400 K, however, the pattern changed significantly. The powder X-ray diffraction pattern of (*R*) isomer-DCA after heating up to 400 K slightly changes. An interesting point is that both patterns of (*S*) isomer-DCA and (*R*) isomer-DCA after heating at 400 K are similar to each other. After heating at each temperature of 323 K, 343 K, 368 K and 398 K, the change in weight was examined. The data are summarized in Table 3. Up to the lower anomaly (~343 K) some solvated molecules were released, and up to the higher anomaly (~398 K) from ~343 K no significant weight loss was observed. In the racemic sample, about 0.7 molecule of MeOH is released at the lower anomaly. These results show that (*S*) isomer-DCA, which includes one molecule of MeOH, releases one solvated molecule at the lower anomaly, and then at the higher anomaly the crystal structure changes to become a structure similar to the (*R*) isomer-DCA heated up to 400 K. The new phase cannot return to the original phase upon cooling, maybe because of a lack of solvated molecules.

All of the $^{57}$Fe Mössbauer spectra showed a ferrocene-like doublet. We found a difference in the $^{57}$Fe Mössbauer spectrum at room temperature among (*S*), (*R*) and racemic isomers-DCA. A measurement of the $^{57}$Fe Mössbauer spectrum of (*S*) isomer-DCA at room temperature did not require a longer time, while measurements of (*R*) isomer-DCA and racemic isomer-DCA required a longer time. According to the Debye approximation at high temperatures, the logarithmic value of

Table 3. Weight Change of (2-Phenylbutyl)ferrocene-DCA

| No. | Condition | (*S*) Isomer/g | Racemic isomer/g |
|---|---|---|---|
| 1 | Before heating | 0.6094 | 1.3538 |
| 2 | After heating up to 323 K | 0.6085 | 1.3530 |
| 3 | After heating up to 343 K | 0.5948 | 1.3270 |
| 4 | After heating up to 368 K | 0.5922 | 1.3264 |
| 5 | After heating up to 398 K | 0.5914 | 1.3259 |
| 6 | Weight loss at 343 K (No.1–No.3) | 0.0146 | 0.0268 |
| 7 | Weight loss at 398 K (No.1–No.5) | 0.0180 | 0.0279 |

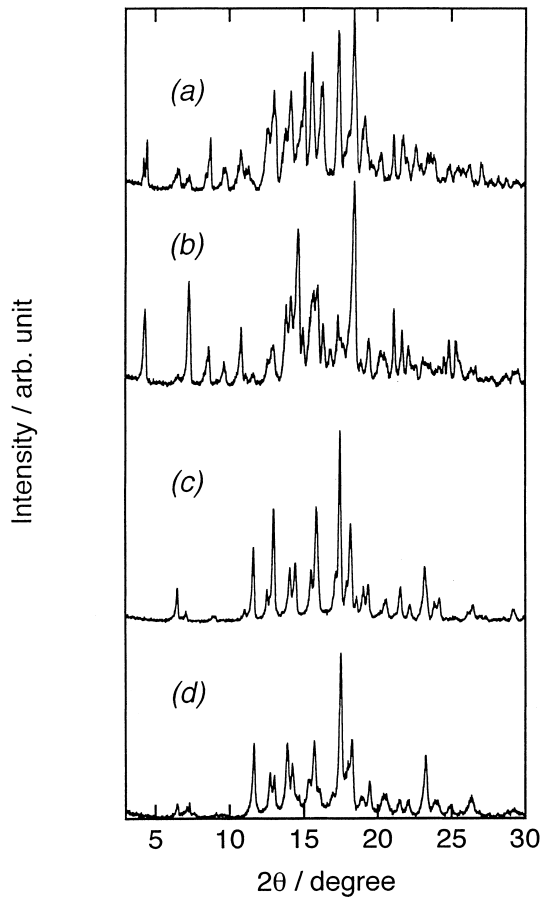


Fig. 7. Powder X-ray diffraction patterns for (a) ((*S*)-2-phenylbutyl)ferrocene-DCA clathrate, (b) sample of (a) after heating up to 343 K, (c) sample of (b) after heating up to 400 K and (d) ((*R*)-2-phenylbutyl)ferrocene-DCA clathrate after heating up to 400 K.

the recoil-free fraction of the $^{57}$Fe Mössbauer spectrum is expected to decrease linearly with increasing temperature. When the sample is thin, the area intensity can be substituted for the recoil-free fraction. The temperature dependences of the area intensity relative to the values at 80 K for (*R*)-, (*S*)- and racemic **3**-DCA clathrates are shown in Fig. 8. The value at room temperature was omitted because the geometry for the measurement was different from the rest. The logarithmic value for the (*S*) isomer-DCA decreases linearly with increasing temperature. On the other hand, the slope for the (*R*) isomer-DCA is similar to that for the (*S*) isomer-DCA from 80 to

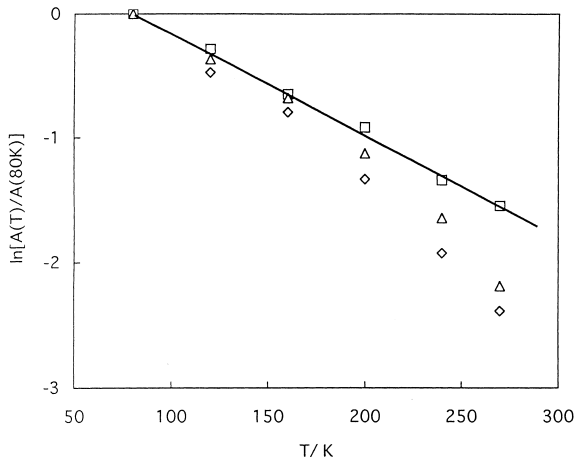


Fig. 8. Temperature dependence of area intensity normalized by the value at 80 K of (2-phenylbutyl)ferrocene-DCA clathrate: □, (*S*) isomer-DCA; △, (*R*) isomer-DCA; ◇, racemic isomer-DCA.

~160 K, while the slope becomes steeper over ~160 K, suggesting that there is a change in the lattice vibrations around ~160 K for the (*R*) isomer-DCA. An interesting point is that the slope for racemic isomer-DCA is not intermediate between (*S*) isomer-DCA and (*R*) isomer-DCA, but is steeper than those of (*S*) isomer-DCA and (*R*) isomer-DCA. These findings suggest that the coexistence of the (*S*) and (*R*) isomers in DCA makes the lattice looser. It is also considered that the (*S*) isomer is tightly packed by the incorporation of MeOH.

It can be concluded that there is an apparent difference in interaction between the guest and host molecules among the (*S*) isomer-DCA, (*R*) isomer-DCA and racemic isomer-DCA for **3**. The (*S*) isomer and MeOH molecule fit very well in the DCA lattice. The good fitness suppresses the molecular motion of ferrocene derivatives in the DCA lattice. On the other hand, the (*R*) isomer is loosely fitted in the DCA lattice and the lattice vibration changes over ~160 K. The looser fit in the racemic isomer-DCA is observed maybe because of the coexistence of (*S*) isomer and (*R*) isomer and partial MeOH molecules in DCA.

## Conclusion

$^{57}$Fe Mössbauer spectroscopy revealed a difference in the interaction between guest and host molecules among the (*R*)-, (*S*)- and racemic isomers for **1** and **3** enclathrated in DCA. The difference in inclusion phenomena between (*R*) and (*S*)

isomers in **2** into the DCA lattice is first observed. $^{57}$Fe Mössbauer spectroscopy combined with X-ray structural analysis will have an important role on the study of a chiral compound in a host lattice having asymmetric carbon. An interesting phase transition was also observed in (*S*) and racemic isomers of **3**-DCA clathrates by using DTA and powder X-ray diffraction patterns, which was accompanied by desolvation and a change of the crystal structure.

## References

1 E.g.; A. Botsi, K. Yannakopoulou, E. Hadjoudis, and B. Perly, *J. Chem. Soc., Chem. Commun.*, **1993**, 1085; A. Botsi, B. Perly, and E. Hadjoudis, *J. Chem. Soc., Perkin Trans. 2*, **1997**, 89.

2 E. Giglio, in "Inclusion Compounds," Academic Press, London (1984), Vol. 2 pp. 207–259.

3 M. Miyata, M. Shibakami, and K. Takemoto, *J. Chem. Soc., Chem. Commun.*, **1988**, 655; K. Miki, N. Kasai, N. Shibakami, K. Takemoto, and M. Miyata, *J. Chem. Soc., Chem. Commun.*, **1991**, 1757.

4 K. Sada, T. Maeda, and M. Miyata, *Chem. Lett.*, **1996**, 837.

5 N. N. Greenwood and T. C. Gibb, in "Mössbauer Spectroscopy," Chapman and Hall, London (1971).

6 S. Nakashima, M. Nakashita, and H. Sakai, *Chem. Lett.*, **1996**, 927.

7 F. Imashiro, N. Kitazaki, D. Kuwahara, T. Nakai, and T. Terao, *J. Chem. Soc., Chem. Commun.*, **1991**, 85.

8 S. Nakashima, H. Komatsu, M. Nakashita, and T. Okuda, *Hyperfine Interact. C*, **3**, 121 (1998); S. Nakashima, N. Ichikawa, H. Komatsu, K. Yamada, and T. Okuda, *Polyhedron*, **19**, 205 (2000).

9 K. Miki, N. Kasai, H. Tsutsumi, M. Miyata, and K. Takemoto, *J. Chem. Soc., Chem. Commun.*, **1987**, 545.

10 M. Miyata, "Chemistry Aiming at Supramolecules," in Kikan Kagaku Sosetsu No. 31, Gakkai Shuppan Center, Tokyo (1997), pp. 217–227.

11 V. I. Gol′danskii, E. F. Makarov, and V. V. Khrapov, *Phys. Lett.*, **3**, 334 (1963).

12 S. V. Karyagin, *Dokl. Akad. Nauk SSSR*, **148**, 1102 (1963).

13 R. L. Collins, *J. Chem. Phys.*, **42**, 1072 (1965).

14 R. M. G. Roberts and J. Silver, *J. Organomet. Chem.*, **263**, 235 (1984).

15 P. Gütlich, R. Link, and A. Trautwein, in "Mössbauer Spectroscopy and Transition Metal Chemistry," Springer, Berlin (1978).